Molecular Biology of the Cell
Vol. 8, 1219–1232, July 1997

Mitogen-activated Protein Kinase/Extracellular Signal-regulated Kinase 2 Regulates Cytoskeletal Organization and Chemotaxis via Catalytic and Microtubule-specific Interactions

Alfred A. Reszka,*† J. Chlöe Bulinski,‡ Edwin G. Krebs,§‖ and Edmond H. Fischer*

Departments of *Biochemistry and §Pharmacology, University of Washington, Seattle, Washington 98195; and ‡Department of Anatomy and Cell Biology, Columbia University, College of Physicians and Surgeons, New York, New York 10032

Submitted January 7, 1997; Accepted April 24, 1997
Monitoring Editor: Tom Pollard

The extracellular signal-regulated kinases (ERKs) 1 and 2 are mitogen-activated protein kinases that act as key components in a signaling cascade linking growth factor receptors to the cytoskeleton and the nucleus. ERK2 mutants have been used to alter cytoskeletal regulation in Chinese hamster ovary cells without affecting cell growth or feedback signaling. Mutation of the unique loop L6 (residues 91–95), which is in a portion of the molecule that is cryptic upon the binding of ERK2 to the microtubules (MTs), generated significant morphological alterations. Most notable phenotypes were observed after expression of a combined mutant incorporating changes to both L6 and the TEY phosphorylation lip, including a 70% increase in cell spreading. Actin stress fibers in these cells, which normally formed a single broad parallel array, were arranged in three or more orientations or in fan-like arrays. MTs, which ordinarily extend longitudinally from the centrosome, spread radially, covering a larger surface area. Single, but not the double, mutations of the Thr and Tyr residues of the TEY phosphorylation lip caused a ca. 25% increase in cell spreading, accompanied by a threefold increase in chemotactic cell migration. Mutation of Lys-52 triggered a 48% increase in cell spreading but no alteration to chemotaxis. These findings suggest that wild-type ERK2 inhibits the organization of the cytoskeleton, the spreading of the cell, and chemotactic migration. This involves control of the orientation of actin and MTs and the positioning of focal adhesions via regulatory interactions that may occur on the MTs.

INTRODUCTION

The cellular response to growth factors and extracellular signals requires a cascade of events leading to the transmission of signals from the cell surface to the cytoskeleton, the nucleus, and other points within the cell. The extracellular signal-regulated kinases, ERK1 and ERK2, representing one type of mitogen-activated protein kinase (MAPK), form a link between the cell surface and these intracellular targets. An obvious role for the ERK signaling cascade is in regulating cell growth and differentiation. In this capacity these ERKs translocate to the nucleus after activation, where they phosphorylate and regulate a number of transcription factors including Elk-1 (reviewed in Karin, 1995).

In most cases, growth factors also effect changes in cytoskeletal architecture leading to altered morphology and chemotactic migration. During cell adhesion and migration, the forward locomotion of the plasma membrane requires the polymerization and cross-link-

† Present address: Department of Bone Biology and Osteoporosis Research, Merck Research Laboratories, West Point, PA 19486.
‖ Corresponding author.

ing of actin (reviewed in Stossel, 1993). Ultimately, focal adhesions are formed that tether actin fibers to the substratum. Cdc42Hs, Rac1, and RhoA are small G-proteins implicated in promoting the formation of novel focal adhesions and the polymerization of actin through sequential events at the plasma membrane (Ridley and Hall, 1992; Ridley *et al.*, 1992; Nobes and Hall, 1995). The ERKs are also activated during cell adhesion via integrin signaling through $pp125^{FAK}$ or caveolin and Shc (Chen *et al.*, 1994; Wary *et al.*, 1996) and during chemotaxis by chemoattractants such as *N*-formylmethionylleucylphenylalanine (Grinstein and Furuya, 1992). In both cases, these signals are transmitted *via* Ras to the ERK/MAPK cascade (Worthen *et al.*, 1994; Clark and Hynes, 1996; Pillinger *et al.*, 1996). However, unlike with the other small G-proteins, signaling through Ras to the ERKs is not required for focal adhesion formation or actin polymerization (Clark and Hynes, 1996; Joneson *et al.*, 1996). Instead, a growing body of evidence suggests that the ERKs may have an inhibitory effect on cytoskeletal organization during these events, possibly through regulation of microtubules (MTs).

In various systems, the ERKs have been shown to associate with either the MTs or the actin filaments. In smooth muscle cells, activated ERK translocates to actin fibers where it is juxtaposed with caldesmon (Khalil *et al.*, 1995). Caldesmon is a substrate for ERK in vitro and phosphorylation of its target sequence has been implicated in the regulation of myosin-MgATPase activity (Childs *et al.*, 1992; Redwood *et al.*, 1993). In neuronal and fibroblastic cells, ERKs 1 and 2 associate with the MTs (Mandelkow *et al.*, 1992; Fiore *et al.*, 1993; Lu *et al.*, 1993; Reszka *et al.*, 1995; Morishima-Kawashima and Kosik, 1996). In cultured fibroblasts, half of all activated ERK is associated with MTs (Reszka *et al.*, 1995), whereas in neuronal cells, the MT-associated pool is constitutively active (Morishima-Kawashima and Kosik, 1996). This places active ERK in close proximity to two MT-associated proteins (MAPs): MAP2, which is found in neuronal tissues, and MAP4, which is nearly ubiquitous. These MAPs stimulate the nucleation of new MTs from $\alpha\beta$-tubulin dimers and promote further polymerization of existing MTs (Herzog and Weber, 1978; Bulinski and Borisy, 1980). However, when MAPs 2 and 4 are phosphorylated by ERK in vitro, these MT-promoting properties are lost (Hoshi *et al.*, 1992).

Studies demonstrating the role of the ERK/MAPK signaling cascade in mitogenesis have also presented evidence of cytoskeletal regulation in vivo (Cowley *et al.*, 1994; Mansour *et al.*, 1994; Seger *et al.*, 1994). Mutants of one type of MAPK kinase, known as MEK (MAPK/ERK Kinase), with constitutive or heightened catalytic activity caused enhanced ERK activity and faster growth rates. These phenotypes were accompanied by morphological rounding and a loss of cytoskeletal organization. In contrast, inactive MEK mutants led to inhibited ERK activities, suppressed growth rates, and enhanced cytoskeletal organization and morphological flattening. Comparable effects were observed with overexpression of a MAPK phosphatase (Noguchi *et al.*, 1993). Furthermore, dominant negative Ras, which inhibits signaling into the ERK cascade by $pp125^{FAK}$, enhanced the formation of novel focal adhesions during cell attachment and spreading (Clark and Hynes, 1996).

The existence of a feedback signaling loop between MEK and Sos, the guanine nucleotide exchange factor for Ras, has complicated our understanding of the ERKs contribution to these cytoskeletal phenotypes. Normally, down-regulation of Ras can be achieved through the phosphorylation of Sos via either ERK or a novel MEK-activated kinase that is not downstream of ERK (Cherniack *et al.*, 1994; Rozakis Adcock *et al.*, 1995; Corbalan-Garcia *et al.*, 1996; Holt *et al.*, 1996). When inactive MEK mutants prevent Sos phosphorylation Ras remains active over a longer period of time. Ras is upstream of a multitude of signaling molecules including Rac1 and RhoA, which have been implicated in cytoskeletal regulation (Ridley and Hall, 1992; Ridley *et al.*, 1992). Thus, an alteration to feedback signaling may contribute to cytoskeletal phenotypes observed in transfectants expressing MEK mutants. Indeed, transient inhibition of Ras activity can partially reverse morphological changes generated through expression of constitutively active MEK, suggesting that feedback signaling adds to the cytoskeletal phenotypes (Cowley *et al.*, 1994).

This report focuses on the role of the ERKs in regulating the cytoskeleton in vivo. Our approach differed from previous studies in that cytoskeleton structure was altered without simultaneously changing cell growth or feedback signaling to Sos. This was achieved by expressing ERK2 mutants at levels below those needed to suppress mitogenesis (Pagès *et al.*, 1993). Our findings suggest that wild-type ERK controls cell morphology and chemotactic migration via mechanisms that control orientation of actin fibers and MTs and the positioning of focal adhesions. In addition to implicating enzyme activation, we found evidence that a unique loop, L6 (Zhang *et al.*, 1994), which is in a region of the protein that is masked when ERK2 is associated with the MTs (Reszka *et al.*, 1995), is necessary for ERK-mediated cytoskeletal regulation. Since catalytically active L6 loop mutants are capable of altering cytoskeletal organization, this implicates ERK–MT interactions in the regulation of cytoskeletal organization within the cell.

MATERIALS AND METHODS

Cells, cDNA Constructs, and Transfections

Chinese hamster ovary (CHO) 10001a cells (a kind gift from Fernando Cabral, University of Texas, Houston, TX) were maintained

in DMEM supplemented with 10% fetal calf serum (FCS) and 2 mM proline and grown in a 5% CO_2/95% air atmosphere. Cells were transfected with 1 μg of plasmid DNA by using the Lipofectin reagent (Life Technologies, Gaithersburg, MD) according to manufacturer's instructions. Stable transfectants were isolated and screened as described (Seger *et al.*, 1994). Hemagglutinin-tagged recombinant ERK2 (HA-ERK2) cDNAs (Frost *et al.*, 1994) were cloned into the pcDNA3 expression vector (Invitrogen, Carlsbad, CA) at *Kpn*I and *Xba*I restriction endonuclease sites. Wild-type ERK2; mutants K52R, T183E, and Y185F; and double mutant T183A/Y185F (AEF) were generous gifts from Melanie Cobb (University of Texas, Southwestern Medical Center, Dallas) and have been previously described (Robbins *et al.*, 1993; Frost *et al.*, 1994). Mutation of two adjacent residues, E94D/Q95A, in the L6 loop (residues 91–95; Zhang *et al.*, 1994) was carried out by the polymerase chain reaction (Seger *et al.*, 1994) using antisense ERK2 oligonucleotide (5′-CCATGAGGTCCTGTACTATATATACATCTTTCATCGCGTCAATGGTT-3′) and sense pcDNA3 oligonucleotide (5′-CCCACTGCTTACTGG-CTTATC-3′). The polymerase chain reaction product was cloned into either of two ERK2-pcDNA3 expression constructs by using *Sac*II and *Ppu*MI restriction endonucleases to create "L6DA," which is catalytically active, and "L6DA/AEF," which is catalytically inactive. All mutant cDNA sequences were verified by double-stranded DNA sequencing.

Cell Growth Rates

Population doubling times were determined after growth for 3 d. Cells were seeded into six-well tissue culture plates at 25,000 cells/well. After 66–76 h, cells were released with trypsin and counted by using a hemocytometer.

MAPK Assays

Cells were seeded at 35% of confluence 48 h prior to assay. After 24 h, medium was aspirated and replaced with serum-free DMEM supplemented with 2 mM proline. Immediately before assay, cells were stimulated with 10% FCS for 0 or 15 min. After stimulation, cells were rapidly chilled on ice and rinsed twice with ice-cold phosphate-buffered saline (PBS). Cells were lysed in buffer A (50 mM β-glycerophosphate, pH 7.3, 2 mM $MgCl_2$, 4 mM EGTA, 1 mM Na_3VO_4, 1 μM Microcystin LR, containing leupeptin at 2 μg/ml, aprotinin at 1 μg/ml, and phenylmethylsulfonyl fluoride at 200 μg/ml) containing 0.2% Triton X-100. Lysates were cleared by centrifugation in a microcentrifuge and pellets were discarded. For determination of mutant HA-ERK2 activities, 200 μg of each cell lysate were immunoprecipitated by dilution (1:5) in buffer A containing 0.05% Tween 20, 1 μg of anti-HA monoclonal antibody (12CA5, Boeringer Mannheim, Indianapolis, IN), and 7.5 μl of protein A-Sepharose (Sigma, St. Louis, MO). After incubation overnight at 4°C with agitation, beads were pelleted and washed three times with ice-cold buffer A containing 0.05% Tween 20. Kinase activities were determined in either 9 μl of crude cell lysate (total cellular ERK activity) or 9 μl of immunoprecipitate beads. These were mixed with either 8 μl of buffer A (background activity) or 8 μl of buffer A containing myelin basic protein (MBP) at a concentration of 1 mg/ml, and then 8 μl of buffer R [reaction mixture at threefold concentration: 50 mM β-glycerophosphate, pH 7.3, 30 mM $MgCl_2$, 4.5 mM dithiothreitol, 0.15 mM Na_3VO_4, 6 mM PKI (cyclic AMP-dependent protein kinase inhibitor) peptide (described in Seger *et al.*, 1994), 3.75 mM EGTA, 30 mM calmidazolium, and 2.5 mg/ml bovine serum albumin (BSA)] supplemented with 100 μM [γ-^{32}P]ATP (1000–2000 cpm/pmol) were added. Kinase mixtures were incubated at 30°C for 15 min for assay of crude lysates or 30 min with agitation (1000 rpm) in a Thermomixer (Eppendorf-Netheler-Hinz GmbH, Hamburg, Germany) for immunoprecipitates. Reactions were stopped with 0.5% (final) phosphoric acid. Radioactivity was quantified by spotting 20 μl on phosphocellulose paper (P81, Whatman, Hillsboro, OR), which was washed six times with 0.5% phosphoric acid (over 1 h) and then radioactivity was measured by scintillation.

Cell Morphology

Cell morphology was analyzed by phase-contrast microscopy using a Nikon Diaphot microscope. Photomicrographs were generated representing the various cell populations and these were analyzed three ways: 1) Regions of the cell periphery that were rounded versus flat were distinguished by nature of their unique refractive indices. During phase-contrast microscopy, rounded edges appeared very bright and flat edges were almost indistinguishable from the surrounding medium. For these analyses, approximately 500 cells/transfectant were examined. 2) and 3) Cell peripheries from 100 or more cells/transfectant were traced from digitized images with a Macintosh PowerPC computer using the public domain NIH Image program (written by Wayne Rasband at the U.S. National Institutes of Health and available from the Internet by anonymous ftp from zippy.nimh.nih.gov or on floppy disk from the National Technical Information Service, 5285 Port Royal Rd., Springfield, VA 22161, part number PB93–504868). From these traces, the length of the cell peripheries, the area of the cells, and their lengths and widths (lengths of the major and minor axes of the best fitting ellipse) were determined. Cell spreading was calculated as either the ratio of area to cell perimeter length or as the the width of the cell.

Immunocytochemistry and Immunoblotting

Immunofluorescence staining of prepared cytoskeletons was carried out as described (Reszka *et al.*, 1995) with the following exceptions: Cells were grown on gelatin-coated (1% solution, 15 min at room temperature) glass coverslips in DMEM containing 10% FCS and 2 mM proline for 5 d prior to extraction and fixation. Antibodies used for immunofluorescence have already been described (Reszka *et al.*, 1995) except anti-vinculin monoclonal antibody (Sigma), which was diluted 1:400. Immunofluorescence signals were analyzed with a Bio-Rad MRC 600 confocal microscope. Immunoblotting was performed according to Reszka *et al.* (1995). Anti-ERK/MAPK polyclonal antibody 7884 (Seger *et al.*, 1994) was used at a concentration of 1:10,000 to probe immunoblots. Sos gel shift analyses were performed as described by Holt *et al.* (1996). Anti-Sos monoclonal antibody (Transduction Laboratories, Lexington, KY) was used to probe immunoblots at a concentration of 0.25 μg/ml.

Cell Migration

Chemotactic cell migration assays were performed as described (Bornfeldt *et al.*, 1994) with the following modifications: Polyvinylpyrrolidone-free polycarbonate membranes (8-μm pore size) were coated with fibronectin (20 μg/ml) and fatty acid-free BSA (5 μg/ml) in PBS (based on Grinnell and Feld, 1982) for 60 min at room temperature. Cells were washed twice with PBS containing EDTA (0.27 M) and released with trypsin (0.0025%) in PBS/EDTA for 1 to 2 min at room temperature. Cells were washed three times with a solution of DMEM containing fatty acid-free BSA (0.1 mg/ml) and suspended at a concentration of 10^6 cells/ml. For each mutant, a minimum of three clones (two for Y185F) were assayed in triplicate in three independent experiments, and migrated cells from two microscopic fields were counted (typically ≥54 microscopic fields were assayed per class of mutant). Relative migration rates were determined by first subtracting average migration rates in the absence of platelet-derived growth factor BB (PDGF-BB) and then comparing adjusted values from each class of transfectant to the untransfected controls.

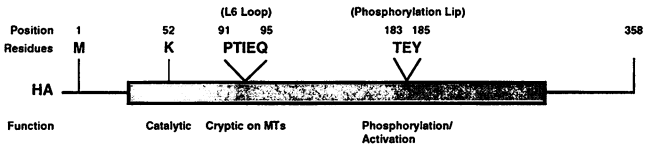

Figure 1. Schematic representation of wild-type HA-tagged ERK2. The amino acid residues targeted for mutation are indicated.

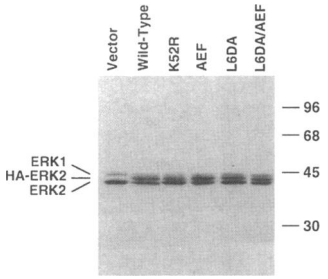

Figure 2. Expression levels of HA-tagged ERK2 in CHO cells. CHO cells were transfected with each of the constructs, isolated, screened for expression, and maintained as described in MATERIALS AND METHODS. After cell lysates were made, proteins were separated by SDS-PAGE, blotted, and probed with an anti-ERK polyclonal antibody.

RESULTS

Expression of HA-tagged ERK2 and Its Mutants in CHO Cells

Manipulation of endogenous ERK activities can be achieved through overexpression of various enzymes that regulate ERK, including mutants of the upstream activator MEK. This is effective in altering ERK activities and cytoskeletal organization, but not without severely altering mitogenesis, oncogenesis, and feedback signaling (Cowley *et al.*, 1994; Mansour *et al.*, 1994; Seger *et al.*, 1994; Holt *et al.*, 1996). To overcome this difficulty, we overexpressed ERK2 and its mutants in CHO cells, which offered a number of benefits: 1) Specific inhibition of ERK activity does not impact feedback signaling to Sos in the CHO cell system (Holt *et al.*, 1996). 2) Inactive ERKs do not suppress mitogenesis without marked overexpression of the mutant enzyme (Pagès *et al.*, 1993). 3) The ERKs bind to the MTs (Mandelkow *et al.*, 1992; Reszka *et al.*, 1995) where they are juxtaposed with cytoskeletal substrates. The normal physical targeting of mutant ERK2 constructs to sites of interaction on the MTs was expected to demonstrate potent cytoskeletal phenotypes.

Figure 1 shows a schematic diagram of ERK2 with the amino acid residues that were targeted for mutation. Lys-52 is necessary for catalytic activity, although it is known that the mutant K52R can be phosphorylated by MEK in vitro and that this generates only 5–7% activity (Robbins *et al.*, 1993). The TEY activation domain (residues 183–185) must be phosphorylated on both Thr and Tyr residues to activate the kinase. The AEF (T183A/Y185F) double mutant is not a substrate for MEK in vitro and is catalytically inactive (Robbins *et al.*, 1993; J. Zhang *et al.*, 1995). In contrast, T183E and Y185F can yield partial activity after in vitro phosphorylation by MEK. We also mutated part of the L6 loop of ERK2 (residues 91–95). L6 contains a unique sequence that resides between subdomains IV and V of ERK2 (Hanks and Hunter, 1995). The crystal structure shows that L6 is adjacent to amino- and carboxyl-terminal epitopes that are masked upon ERK–MT interaction (Zhang *et al.*, 1994; Reszka *et al.*, 1995). The catalytically active "L6DA" mutant (E94D/Q95A) and an inactive variant "L6DA/AEF" (E94D/Q95A/T183A/Y185F) were created to assess the contribution of L6 to cytoskeletal regulation.

Interestingly, regarding the HA-tagged ERK2 constructs, a two- to threefold larger proportion of G418-resistant clones were found to express the catalytically inactive mutants than the wild-type enzyme or the catalytically active L6DA mutant. They all migrated with an apparent molecular weight of 43 kDa by SDS-PAGE and could be visualized by immunoblotting with anti-ERK (Figure 2) or anti-HA antibodies. The anti-ERK antibodies enabled direct comparison between expression of HA-ERK2 and the endogenous enzyme, which migrates at 42 kDa. We chose wild-type and mutant constructs with expression levels near to those of the endogenous enzyme (approximately twofold expression) for further analysis. This was the highest consistent level of expression attained in this system and well below levels expected to alter mitogenesis.

Effect of ERK2 Mutants on Endogenous ERK Activities and Cell Growth

The effects of a twofold overexpression of the ERK2 mutants on mitogenesis was explored (Figure 3). To examine the intrinsic activities of the overexpressed kinases, the epitope-tagged constructs were immunoprecipitated from cell lysates using an anti-HA antibody. Kinase activities were determined by using MBP as a substrate in both in-gel kinase assays, which showed kinase activity in a single band of 43 kDa (our unpublished results), and in suspension with the HA-tagged constructs still attached to the protein A-Sepharose beads (Figure 3A). Comparable 16- and 17-fold increases in activity for the wild-type and the L6DA ERK2 constructs, respectively, were found after serum-starved cells were stimulated with FCS for 15 min. All of the mutants targeting residues required for catalytic activity showed essentially no enzymatic activity after stimulation with FCS for 15 min. Anti-phosphotyrosine immunoblotting showed that the stimulation caused elevated phosphorylation on the

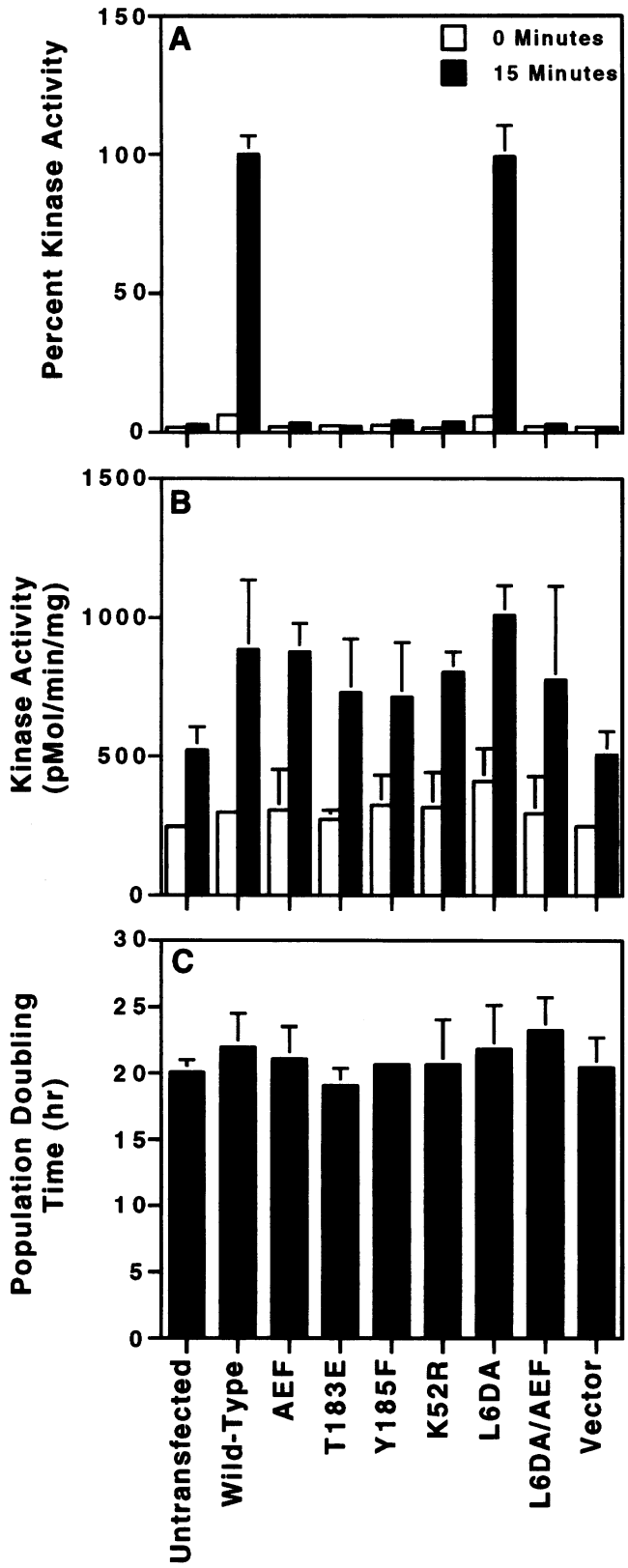

Figure 3.

K52R and T183E constructs, relative to wild-type (or L6DA), and no phosphorylation of Y185F, AEF, or L6DA/AEF (our unpublished results).

We next analyzed total cellular ERK activities in crude lysates after cells were stimulated with FCS for 15 min. Cells expressing the wild-type or L6DA constructs showed 1.7- to 1.9-fold increases in total stimulated activity when compared with untransfected cells or those transfected with the empty vector (Figure 3B). This possibility was predicted because both of these constructs were catalytically active and overexpressed by twofold. Total ERK activities from cells expressing the inactive ERK2 constructs: K52R, T183E, Y185F, AEF, and L6DA/AEF, were 1.5- to 1.8-fold higher than untransfected controls. These data showed that the expressed mutants failed to act as "dominant negative" kinases. Instead, an unexpected but small increase in total activity was observed, which may be due to minor interference with mechanisms involved in negative regulation of the ERKs.

Since twofold expression of inactive ERK2 mutants failed to suppress endogenous kinase activities in the CHO system, we predicted that they would not suppress cell growth. Previous experiments with ERK1 mutants had shown that suppression of mitogenesis required markedly high levels of expression (Pagès *et al.*, 1993). Cell growth was assessed by analyzing population doubling times over a period of 3 d. The results in Figure 3C demonstrate that the inactive kinases K52R, T183E, Y185F, AEF, and L6DA/AEF did not influence cell growth rates: cells grew with an average doubling time of 21 h, which is indistinguishable from those of the untransfected cells and cells transfected with wild-type ERK2 or vector alone. Similarly, cells overexpressing the catalytically active L6DA mutant grew at normal rates.

Figure 3 (cont). Effects of wild-type and mutant ERKs on kinase activities and cell growth. (A and B) ERK kinase activities were determined after cell stimulation for 0 and 15 min with 10% FCS. Cells were grown, stimulated, and prepared as described in MATERIALS AND METHODS. (A) Activities of HA-tagged wild-type and mutant ERKs were assessed by using MBP as a substrate after constructs were immunoprecipitated with an anti-HA antibody (12CA5). Kinase activities are expressed as a percentage of the average activity obtained from wild-type HA-ERK2 after a 15-min stimulation. (B) Total cellular ERK activities (endogenous and overexpressed) were determined by using crude lysates from transfected cells. Activities are expressed as pmol of phosphate transferred to MBP per min per mg of crude cell lysate. (C) Cell growth rates, expressed as population doubling times, were determined over a 3-d period as described in MATERIALS AND METHODS. Kinase activities and growth rates were determined from three independent assays using three independent clones representing each class of transfectant.

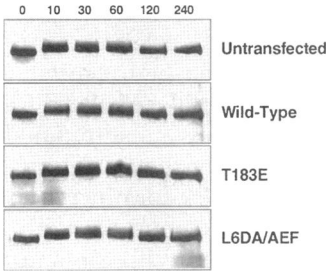

Figure 4. Serum stimulation of Sos phosphorylation in untransfected CHO cells and wild-type and mutant ERK2 transfectants. Cells were stimulated over a 120-min time course and crude lysates were examined for phosphorylation of Sos (apparent molecular weight approximately 170 kDa) by using an SDS-PAGE band-shift analysis. Immunoblots were prepared and probed with an anti-Sos monoclonal antibody as described in MATERIALS AND METHODS.

ERK2 Mutants Do Not Interfere with Feedback Signaling to Sos

One means by which inactive ERK2 mutants might trigger the small increases observed in endogenous kinase activity is via interference with the MEK/Sos feedback loop (Waters *et al.*, 1995). Such interference would prolong Ras signaling into the ERK cascade. Although ERK phosphorylation sites on Sos have been shown to regulate the Grb2–Sos interaction in vitro (Corbalan-Garcia *et al.*, 1996), specific inactivation of ERKs 1 and 2 has been shown to have no impact on Sos phosphorylation during mitogenesis in the CHO cell system (Holt *et al.*, 1996). To confirm this, we determined whether our ERK2 mutants affected feedback signaling to Sos in response to serum stimulation in the CHO transfectants. The phosphorylation of Sos in each of the various transfected cells (Figure 4) was determined by examining alterations in electrophoretic mobility before and after stimulation. Treatment of untransfected CHO cells with 10% FCS for 0, 10, 30, 60, 120, or 240 min (Figure 4A, lanes 1–6) showed that Sos (apparent molecular weight approximately 170 kDa) was rapidly phosphorylated, as seen by a doublet of slower migrating bands during SDS-PAGE. These findings are in slight contrast with results presented for insulin-stimulated CHO/IR cells, which display transient phosphorylation of Sos, lasting for less than 30 min (Waters *et al.*, 1995). A similar phosphorylation profile was also observed in CHO transfectants expressing wild-type enzyme (Figure 4B), T183E (Figure 4C), or L6DA/AEF (Figure 4D). Analyses of all other mutants stimulated for 0, 10, and 30 min with 10% FCS showed comparable changes in electrophoretic mobility (our unpublished results). These data suggest that these ERK mutants do not interfere with feedback signaling to Sos. They are of further significance since they suggest that the cytoskeletal and chemotactic phenotypes described below are attributable to ERK activities and not to other signaling molecules activated as a result of abnormal feedback signaling to Sos and, ultimately, through Ras.

Effect of ERK2 Mutants on Cell Morphology and Cytoskeletal Organization

Unlike ERK2 interactions in the nucleus, which occur in a diffuse pool of enzyme (Reszka *et al.*, 1995), those between ERK2 and MT-associated substrates are predicted to take place within the context of a bound state. Thus, the various mutants may demonstrate cytoskeletal phenotypes by nature of their ability to effectively block interactions between substrate and functional kinases. The observed morphological phenotypes of the ERK transfectants suggested that this had occurred. Untransfected cells showed predominantly elongated fibroblastic or bipolar morphologies (Figure 5A) and the average cell length and widths were at 117 and 12.5 μm, respectively. The latter was used to determine the relative cell widths of the various transfectants (Table 1). A second parameter of cell spreading examined the ratio of cell area to the length of the cell periphery (A/P ratio). The A/P ratio increases as a cell spreads over a wider area. Relative values for the various transfectants are shown in Table 1 and an A/P ratio of 7.8 was determined for the untransfected CHO cells. The somewhat large standard deviations observed in these cell spreading assays was not unexpected, as each cell within a given population displayed a slightly different shape and degree of spreading (Figure 5). Cell perimeters were also examined in terms of the flatness of the edges, which was analyzed by using phase–contrast microscopy, as described in MATERIALS AND METHODS. Ten percent of the untransfected population had completely flattened edges that are almost indistinguishable from the surrounding medium (Figure 5, A and F).

All clones expressing the wild-type ERK2 (Figure 5, B and F) or empty vector (Figure 5F) showed no increases in cell spreading (Table 1) and a comparable proportion of completely flat cells in the population. Notable alterations in cell morphology were observed for most of the clones expressing the L6DA (five of eight) and L6DA/AEF (six of nine) mutants (Figure 5, C and D, respectively). Most striking phenotypes were found in the L6DA/AEF transfectants, which were both larger and flatter than the control cells. These showed a 70% increase in cell spreading, with an average width of 22.5 μm and an average A/P ratio of 12.3 (Table 1). Phase-contrast microscopy showed that the peripheral membranes in these cells also extended to form thinner and flatter edges that were almost indistinguishable from the surrounding medium (Figure 5D, arrows and inset). Populations expressing L6DA/AEF showed a fivefold increase in the number of cells with a completely flattened

periphery (50% of the population) compared with those expressing the controls (Figure 5F). Interestingly, transfectants expressing the catalytically active L6DA mutant displayed morphological differences that were not readily distinguished by quantitative analyses. These cells showed particularly bright cell peripheries (Figure 5C, arrows and inset) and an increase in the number of darkened patches near the cell termini. However, analyses of cell spreading (Table 1) and edge flattening (Figure 5F) showed consistent but minor increases in these parameters. The vast increases in cell spreading and flattening observed after expression of the L6DA/AEF "double" mutant appeared to arise from a synergy between the L6DA mutation and the (TEY to) AEF mutation, which by itself had no qualitative or quantitative effects on cell spreading or flattening (Table 1; Figure 5, E and F). In contrast, two other mutations targeting single residues of the TEY phosphorylation lip, T183E, and Y185F, showed a 20–25% increase in cell spreading (Table 1). This correlated well with a 2.5-fold increase in the number of cells with completely flattened edges (Figure 5F). The K52R mutation demonstrated a larger increase in cell spreading (48% over the controls), with an average width of 19.5 μm and an A/P ratio of 10.7. The K52R populations also showed a 2.5-fold increase in the number of cells with completely flattened cell peripheries.

To examine alterations in the actin and MT networks, cytoskeletons were prepared from cells that were grown on glass coverslips, stained with cytoskeleton-specific antibodies, and analyzed by confocal microscopy (Figures 6 and 7). MTs were stained with both anti-tubulin and anti-ERK antibodies (Figure 6). Actin stress fibers and focal adhesions were visualized with anti-actin and anti-vinculin antibodies, respectively (Figure 7). In untransfected cells both the MT and actin networks were oriented along the long axes of the cells (Figures 6A and 7A). Since the MTs were stained with both anti-tubulin and anti-ERK antibodies, the signals were coincident. In the untransfected (Figure 6A) or vector control cells (Figure 6F), the combined image was orange rather than yellow/green because these cells did not overexpress ERK2. Focal adhesions (Figure 7A), which fluoresce with a green signal from fluorescein isothiocyanate (FITC), are found at the end of the Texas Red-labeled actin stress fibers and were mostly limited to either end of the cell or beneath the nucleus in these control cells.

Similar immunofluorescence patterns were observed for CHO cells overexpressing the wild-type HA-ERK2 constructs, with both cytoskeletal networks oriented along the length of the cells (Figures 6B and 7B). The ERK-specific staining seen in Figure 6 showed an increase in the green signal from FITC label, which combined with the signal from Texas Red-labeled tubulin to yield a more intense yellow/green color. This demonstrated the enhanced levels of MT-bound ERK2 in transfected cells compared with the untransfected or vector controls. The increase in ERK–MT association was also observed for L6DA (Figure 6C), L6DA/AEF (Figure 6D), AEF (Figure 6E), and the other mutants, suggesting that all bound to the MTs in the CHO cell system. This increase appeared qualitatively proportionate to the expression of HA-ERK2 and was verified by cell fractionation (our unpublished results) as previously described (Reszka *et al.*, 1995). In a majority of the cells expressing the L6DA mutant (Figure 6C), the MT networks radiated from the centrosome into lateral regions instead of orienting toward either end of the cell. The actin cytoskeleton was also rearranged (Figure 7C), typically with three sets of arrays, each in a different orientation and with focal adhesions found in three or more clusters along the cell periphery. Cells expressing L6DA/AEF showed a 50%

Table 1. Analyses of cell spreading induced by ERK2 mutants

Designation	A/P ratio[a] (relative value)	Cell width[b] (relative value)	Composite value[c]
Untransfected	7.77 ± 2.59 (1.00 ± 0.33)	12.5 ± 0.6 (1.00 ± 0.50)	1.00
Wild-type	7.75 ± 2.23 (1.00 ±0.29)	12.9 ± 5.3 (1.04 ± 0.42)	1.02
AEF	7.43 ± 3.07 (0.96 ± 0.40)	12.0 ± 6.7 (0.96 ± .055)	0.96
T183E	9.27 ± 2.71 (1.19 ± 0.35)	16.3 ± 7.1 (1.31 ± 0.58)	1.25
Y185F	8.74 ± 3.08 (1.12 ± 0.40)	15.8 ± 8.1 (1.27 ± 0.65)	1.20
K52R	10.7 ± 4.0 (1.37 ± 0.52)	19.6 ± 9.1 (1.58 ±0.73)	1.48
L6DA	8.44 ± 2.06 (1.09 ± 0.27)	13.9 ± 5.3 (1.12 ± 0.42)	1.11
L6DA/AEF	12.3 ± 3.9 (1.58 ± 0.50)	22.5 ± 8.1 (1.81 ± 0.65)	1.70
Vector	7.23 ± 2.10 (0.93 ± 0.27)	12.0 ± 5.8 (0.96 ± 0.46)	0.95

Cell perimeters of approximately 100 cells per transfectant were traced and the following were measured: area, perimeter length, and width, as described in MATERIALS AND METHODS.

[a] A/P (area/perimeter length) ratios were determined for each cell type (mean ± SD) and increase with greater spreading.

[b] Cell widths in μm (mean ± SD) were determined from the same population of cells by measuring the length of the minor axis of the best-fitting ellipse for each cell.

[c] Composite values are the average of relative A/P ratio and cell width values.

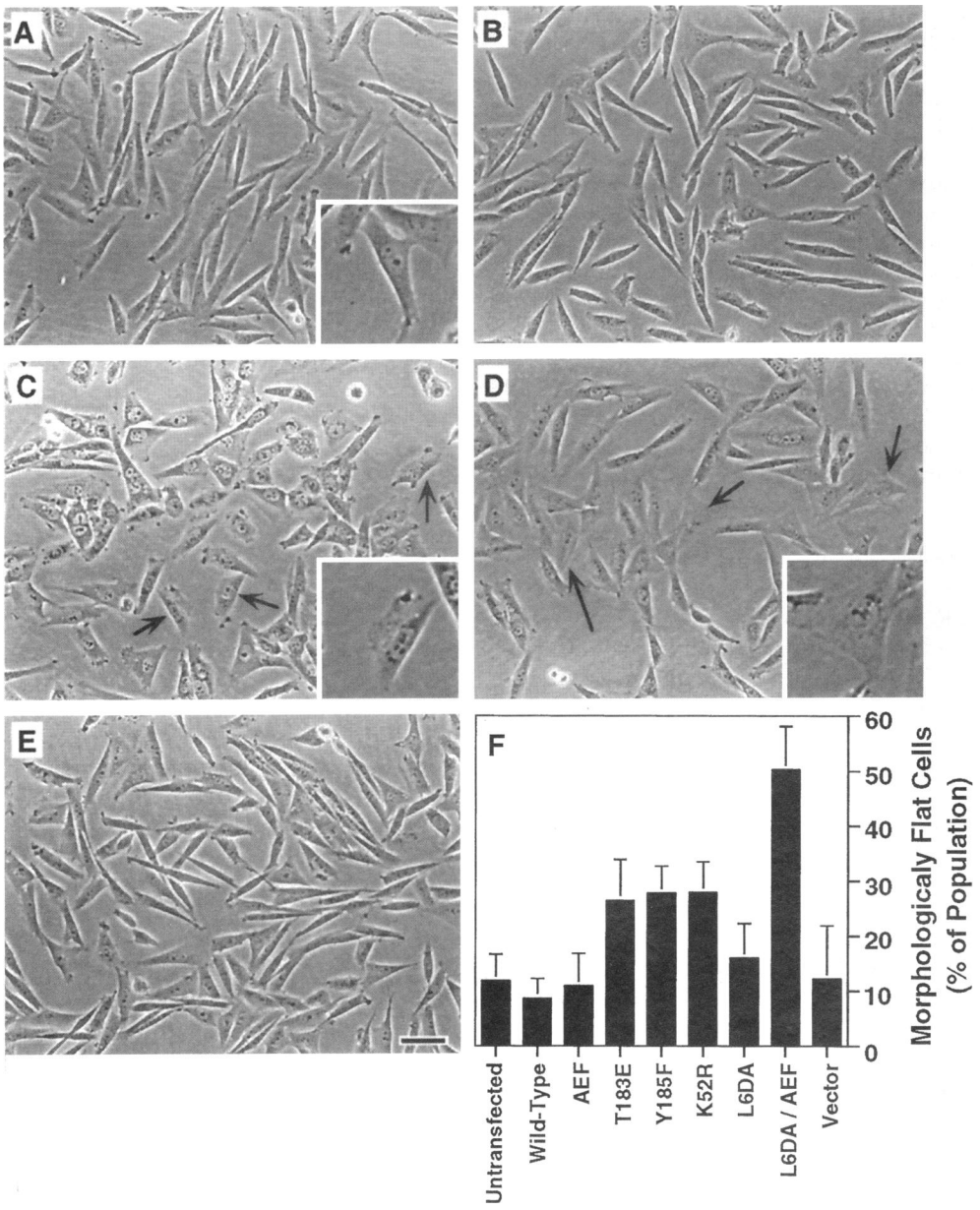

Figure 5. Morphological alterations induced by overexpression of the L6DA ERK2 constructs. Cells were grown on tissue culture plastic and photographed during phase-contrast microscopy. (A–E) Cells are untransfected (A), wild-type ERK2 (B), L6DA (C), L6DA/AEF (D), and AEF (E). Bar, 50 μm. (A, C, and D, Insets) Micrographs are magnified an additional 2×. (F) Cells were counted from populations of three independent clones representing each of the various transfectants (approximately 500 cells for each transfectant). Values represent the percentage of cells with completely flat edges.

increase in spreading over those expressing L6DA (Table 1). The MT arrays in these transfectants extended radially throughout the cytoplasm, terminating at multiple points along the cell periphery. The actin arrays in L6DA/AEF cells (Figure 7D) were in multiple orientations or fan-like arrays. Similar but less-extensive cytoskeletal rearrangements were observed in 25% of all cells expressing the K52R, T183E, and Y185F mutants. These changes included reorientation of the actin cytoskeleton and enhanced spreading of MTs and were consistent with the 20–50% increases in cell spreading. None of the mutant ERK2 constructs appeared to alter the number of Glu-MTs or the sensitivity of the MTs to disruption with nocodazole (our unpublished results). Changes in the actin and MT arrays did not appear to result from an in-

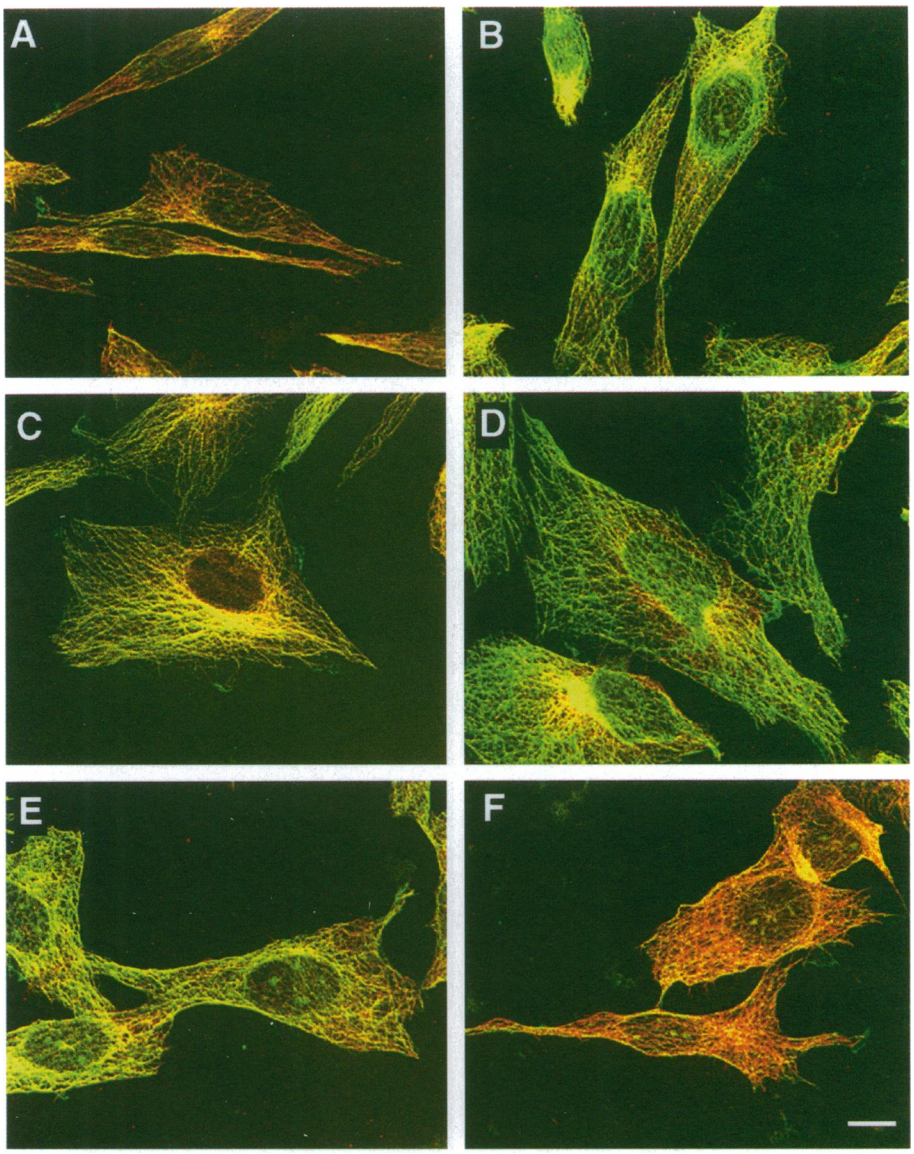

Figure 6. Microtubule organization and overexpression of ERK2 on MTs in untransfected CHO cells and wild-type and mutant ERK2-transfectants. Cytoskeletons were prepared, immunofluorescently stained with anti-tubulin pAB(X^2) (Texas Red) and pan-ERK monoclonal antibody (Transduction Laboratories; FITC) and analyzed with confocal microscopy as described in MATERIALS AND METHODS. Cells are untransfected (A), wild-type ERK2 (B), L6DA (C), L6DA/AEF (D), AEF (E), and vector (F). Bar, 10 μm.

crease in the overall quantity of polymer, as determined by immunohistochemistry and cell fractionation (Figures 6 and 7 and our unpublished results), thus suggesting that the predominant phenotype related to the orientation and positioning of these arrays.

ERK2 Mutants Enhance Chemotactic Cell Migration

A possible link between the ERKs and cell migration has already been suggested by their activation after stimulation with chemoattractants such as *N*-formylmethionylleucylphenylalanine (Thompson *et al.*, 1993; Pillinger *et al.*, 1996). Since the ERK mutants described herein caused significant morphological and cytoskeletal changes, we hypothesized that chemotaxis toward PDGF-BB might also be affected. Cell migration of multiple wild-type- and mutant-expressing clones were assessed in triplicate in three independent experiments, and relative migration rates were determined (Figure 8) as described in MATERIALS AND METHODS. These analyses were performed with multiple clones representing each of the various transfectants. There-

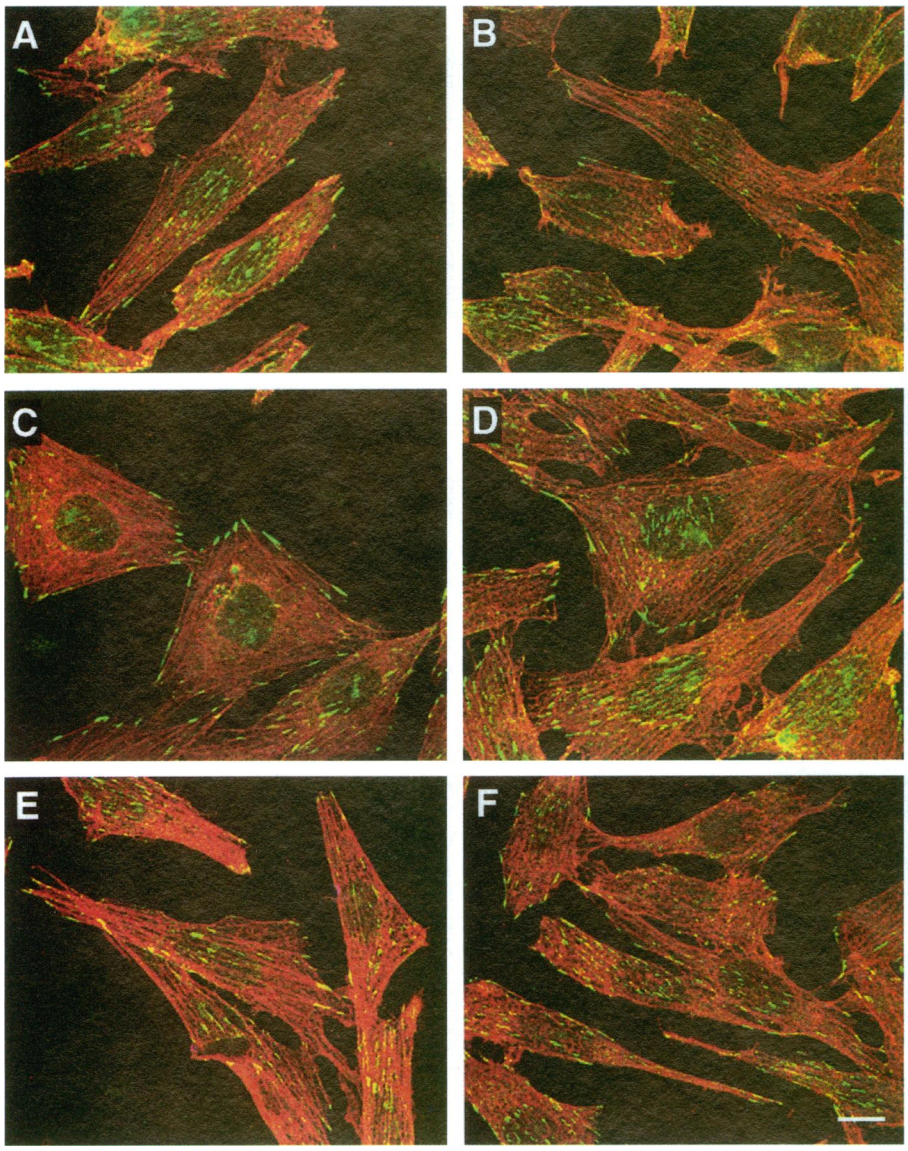

Figure 7. Actin organization in untransfected CHO cells and wild-type and mutant ERK2 transfectants. Cytoskeletons were prepared and stained as in Figure 6 using anti-actin pAB(G^2) (Texas Red) and anti-vinculin monoclonal antibody (Sigma; FITC). Cells are untransfected (A), wild-type ERK2 (B), L6DA (C), L6DA/AEF (D), AEF (E), and vector (F). Bar, 10 μm.

fore, the standard deviations observed in these analyses reflect differences stemming from clonal variation rather than inconsistencies within each population. Cells expressing the wild-type ERK2 construct migrated at an average twofold higher rate than the untransfected control cells in response to PDGF-BB. Similar or lesser migration rates were observed for vector transfectants and cells expressing four of six ERK2 mutants. Cells expressing T183E or Y185F showed significantly higher (approximately threefold) rates in cell migration relative to the untransfected control cells. These results were remarkable because of their comparability in generating near identical rates of migration and in targeting only single residues in the phosphorylation lip of ERK2. In contrast, AEF, which targets both hydroxyl-bearing residues, migrated at nearly identical rates to those of the untransfected control cells. This suggests that these phenotypes may be generated by both regulation of catalytic activity and the conformational state of the enzyme.

DISCUSSION

A fundamental question in signal transduction research regards the distribution of information be-

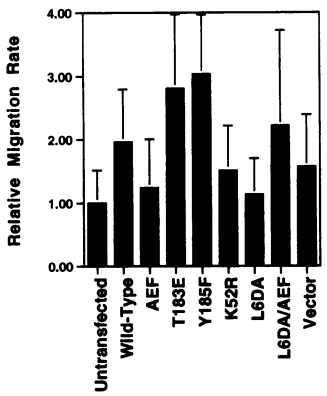

Figure 8. Chemotactic cell migration toward PDGF-BB. For each clone, cells were prepared and added to the top of the chemotaxis chambers and migrated toward PDGF-BB (30 ng/ml), which was loaded in the lower chambers. After a 4-h incubation at 37°C, migrated cells were stained and quantified by microscopy. Relative migration values were determined by comparing averaged values to those from untransfected controls as described in MATERIALS AND METHODS.

tween different subcellular compartments. Four small G-proteins within the Ras family are implicated in regulating the cytoskeleton and transcription. Cdc42Hs, Rac1, and RhoA initially emerged as regulators of the cytoskeleton and subsequently were found to regulate transcription through the JNK and p38 MAPK cascades (Bagrodia *et al.*, 1995; Coso *et al.*, 1995; Minden *et al.*, 1995; S. Zhang *et al.*, 1995). Ras has long been known to affect both oncogenesis and cytoskeletal integrity. After discovery of the first MAPK signaling pathway the ERKs were identified as elements downstream of Ras capable of both cytoskeletal and mitogenic regulation (Hoshi *et al.*, 1992; Pagès *et al.*, 1993). Numerous other studies also implicate the ERKs in regulating the MTs (Gotoh *et al.*, 1991; Drechsel *et al.*, 1992; Shiina *et al.*, 1992; Lu *et al.*, 1993; Verlhac *et al.*, 1993, 1994, 1996). Some studies have shown that the ERKs have no ability to promote the polymerization of actin or the formation of focal adhesions, leading to the conclusion that they do not regulate the cytoskeleton or cellular morphogenesis in vivo (Clark and Hynes, 1996; Joneson *et al.*, 1996). A number of possibilities might explain how mutants of Ras, Raf1, MEK, and ERK alter cytoskeletal organization and cell morphology including the facts that 1) the ERKs directly regulate cytoskeletal elements such as the MAPs, 2) feedback signaling through Ras leads to activation of other relevant pathways, and 3) downstream targets associated with mitogenesis can be implicated. This report demonstrates that ERK2 regulates cytoskeletal organization and chemotactic cell migration independently of its effect on mitogenesis or feedback signaling that would ultimately affect Ras. This is of importance, because the described phenotypes suggest that the ERKs regulate the cytoskeleton in response to mitogenic and chemotactic signals. As such, the ERKs play a significant role in establishing a necessary balance between forces that promote or restrict the organization of the cytoskeleton.

The ERKs are present in three identifiable subcellular pools in fibroblasts: MT-bound, diffuse cytoplasmic, and diffuse nuclear (Reszka *et al.*, 1995). Our data suggest that the MT-bound ERKs are responsible for regulating cytoskeletal organization. The specificity of the L6 mutants for generating cytoskeletal phenotypes suggests that the ERKs regulate the cytoskeleton via interactions that may occur on the MTs. The importance of the findings relates to the fact that this loop does not contribute to catalysis, and it resides in a region of the molecule that is cryptic upon ERK2 binding to the MTs. Mutations that affect either the L6 loop (L6DA) or both the L6 loop and enzyme activation (L6DA/AEF) drastically altered the general organization of the cytoskeleton in the cell but had no effect on growth or feedback signaling to Sos, both of which are considered to be regulated in noncytoskeletal compartments. The cell spreading and flattening in the L6DA/AEF transfectants was not as marked as in cells with massively suppressed ERK activities as seen after overexpression of dominant negative MEK (Cowley *et al.*, 1994; Seger *et al.*, 1994). However, unlike in the previous studies, the phenotypes observed with the ERK2 mutants were generated with modest overexpression of the enzyme and in the absence of other mitogenic phenotypes. Furthermore, cytoskeletal and morphological phenotypes were observed without targeting the catalytic activity of the enzyme, as occurred with the L6 loop (L6DA) mutant. Thus MT-specific interactions correlate with cytoskeleton-specific phenotypes.

It is still not known what ERK2 is interacting with via the L6 loop, because both L6DA mutants bound to the MTs as seen by both immunofluorescent staining and by cell fractionation. Morishima-Kawashima and Kosik (1996) have shown that ERK2 and MAP2 associate in vitro, an interaction that may occur via L6. However, MAP2 is not found in tissues or cells of nonneuronal origin. While MAP4 is also a candidate, its function in the cell is unclear because disruption of the MAP4–MT interaction has been shown to have no effect on MT distribution in vivo (Wang *et al.*, 1996). Furthermore, we have observed that ERK2 binds directly to MTs in vitro and that its binding is not altered by the addition of MAP4 or a synthetic L6 peptide (Reszka and Bulinski, unpublished observations). Certainly our understanding of the mechanism by which the L6 loop mutants act would benefit from the identification of relevant substrates and proteins that might interact with this region of the molecule.

Previous crystallographic analyses may provide insight as to why the various inactive ERK2 mutants

generated different phenotypes. Mutations targeting K52, T183, and Y185 do not significantly disorder the L6 loop (residues 91–96), which resides on the surface of the enzyme above the catalytic pocket (Zhang *et al.*, 1994; J. Zhang *et al.*, 1995; Robinson *et al.*, 1996). This may explain why the L6 mutants can generate unique cytoskeletal rearrangements. Our results also show that the ERKs regulate chemotactic cell migration perhaps through interactions that would not involve the L6 loop. Two mutants (T183E and Y185F) targeting the TEY motif within the phosphorylation lip caused modest increases in morphological flattening and threefold increases in chemotactic cell migration toward PDGF-BB. Surprisingly, however, a double mutant targeting both T183 and Y185 (AEF) had no effect on morphology or chemotaxis. The AEF mutation induced high levels of disorder (B-factor shifts) in at least five regions of the molecule, based on a comparable mutant simultaneously targeting both T183 and Y185 (J. Zhang *et al.*, 1995). In contrast, T183E caused only a modest level of disorder in the phosphorylation lip and Y185F only in the phosphorylation lip and a portion of subdomain II. It is possible, therefore, that moieties disrupted by the AEF double mutation are critical in generating the chemotactic phenotype. One putative sequence (loop L14) is unique to the ERKs, is disrupted by a double mutation of TEY, and is adjacent to an epitope (residues 305–325) that is cryptic upon the ERK–MT interaction (Zhang *et al.*, 1994; Reszka *et al.*, 1995).

A second possible factor that differentiates the phenotypes associated with each particular ERK2 mutant relates to their phosphorylation by MEK. Simultaneous phosphorylation of T183 and Y185 is sufficient and necessary to trigger the opening the catalytic pocket, which is shifted by 17° when compared with that of active cyclic AMP-dependent protein kinase (Zhang *et al.*, 1994). No information is available regarding the crystal structure of the ERKs or their mutants after phosphorylation by MEK. However, we and others have shown that MT-associated ERKs are highly phosphorylated on tyrosine and more active than their soluble counterparts (Lu *et al.*, 1993; Reszka *et al.*, 1995; Morishima-Kawashima and Kosik, 1996). Because each of the ERK mutants bound to the MTs with apparently equal affinity, this may suggest that phosphorylation plays an important role in regulating ERK interactions after binding to the MTs. In this respect, there exists three classes of (non-L6) mutants that are all catalytically inactive but discernible by their level of phosphorylation. K52R can be fully phosphorylated by MEK and produced a 2.5-fold increase in morphological flattening but no changes in chemotaxis. T183E and Y185F can still be partially activated after phosphorylation on a single residue by MEK in vitro (J. Zhang *et al.*, 1995). These mutants also cause threefold increases in chemotaxis and 2.5-fold increases in flattening of the cells. Finally, the AEF mutant is excluded as a possible candidate for phosphorylation by MEK; it was not detected by anti-phosphotyrosine antibodies after stimulation with FCS and generated no discernible phenotype.

The evidence suggests that ERK2 regulates cytoskeletal organization and chemotaxis through distinct interactions that may occur within the context of enzyme–substrate contacts formed on the MTs. Previous data had shown that inactive ERKs cannot suppress mitogenesis in the absence of a marked overexpression of the enzyme. In agreement with this, it was shown that a twofold expression of mutant ERK2 had no effect on cell growth rates or feedback inhibition. Instead, the only discernible phenotypes were those that involved the regulation of cytoskeletal organization and chemotaxis. Although no clear mechanism can yet be proposed, one can assume that phosphorylation, catalytic activity, and MT-specific interactions might be implicated. One may wonder whether a more significant rearrangement of the cytoskeleton after high level overexpression of ERK or MEK mutants might also significantly affect cell growth regulation.

ACKNOWLEDGMENTS

We thank Melanie Cobb for the gift of ERK2 cDNA constructs and Fernando Cabral for the parental CHO cell line. We also thank Paulette Brunner and the W.M. Keck Center for Advanced Studies in Neural Signaling for assistance with confocal microscopy. This work was supported by National Institutes of Health grants DK-07902 and DK-42528. A.A.R. was supported, in part, by a fellowship from the Jane Coffin Childs Memorial Fund for Medical Research.

REFERENCES

Bagrodia, S., D'Erijard, B., Davis, R. J., and Cerione, R. A. (1995). Cdc42 and PAK-mediated signaling leads to Jun kinase and p38 mitogen-activated protein kinase activation. J. Biol. Chem. *270*, 27995–27998.

Bornfeldt, K.E., Raines, E.W., Nakano, T., Graves, L.M., Krebs, E.G., and Ross, R. (1994). Insulin-like growth factor-I and platelet-derived growth factor-BB induce directed migration of human arterial smooth muscle cells via signaling pathways that are distinct from those of proliferation. J. Clin. Invest. *93*, 1266–1274.

Bulinski, J.C., and Borisy, G.G. (1980). Microtubule-associated proteins from cultured HeLa cells. Analysis of molecular properties and effects on microtubule polymerization. J. Biol. Chem. *255*, 11570–11576.

Chen, Q., Kinch, M.S., Lin, T.H., Burridge, K., and Juliano, R.L. (1994). Integrin-mediated cell adhesion activates mitogen-activated protein kinases. J. Biol. Chem. *269*, 26602–26605.

Cherniack, A.D., Klarlund, J.K., and Czech, M.P. (1994). Phosphorylation of the Ras nucleotide exchange factor son of sevenless by mitogen-activated protein kinase. J. Biol. Chem. *269*, 4717–4720.

Childs, T.J., Watson, M.H., Sanghera, J.S., Campbell, D.L., Pelech, S.L., and Mak, A.S. (1992). Phosphorylation of smooth muscle caldesmon by mitogen-activated protein (MAP) kinase and expression of MAP kinase in differentiated smooth muscle cells. J. Biol. Chem. *267*, 22853–22859.

Clark, E.A., and Hynes, R.O. (1996). Ras activation is necessary for integrin-mediated activation of extracellular signal-regulated kinase 2 and cytosolic phospholipase A2 but not for cytoskeletal organization. J. Biol. Chem. *271*, 14814–14818.

Corbalan-Garcia, S., Yang, S.-S., Degenhardt, K.R., and Bar-Sagi, D. (1996). Identification of the mitogen-activated protein kinase phosphorylation sites on human Sos1 that regulate interaction with GRB2. Mol. Cell. Biol. *16*, 5674–5682.

Coso, O.A., Chiariello, M., Yu, J.C., Teramoto, H., Crespo, P., Xu, N., Miki, T., and Gutkind, J.S. (1995). The small GTP-binding proteins Rac1 and Cdc42 regulate the activity of the JNK/SAPK signaling pathway. Cell *81*, 1137–1146.

Cowley, S., Paterson, H., Kemp, P., and Marshall, C.J. (1994). Activation of MAP kinase kinase is necessary and sufficient for PC12 differentiation and for transformation of NIH 3T3 cells. Cell *77*, 841–852.

Drechsel, D.N., Hyman, A.A., Cobb, M.H., and Kirschner, M.W. (1992). Modulation of the dynamic instability of tubulin assembly by the microtubule-associated protein tau. Mol. Biol. Cell *3*, 1141–1154.

Fiore, R.S., Bayer, V.E., Pelech, S.L., Posada, J., Cooper, J.A., and Baraban, J.M. (1993). p42 mitogen-activated protein kinase in brain: prominent localization in neuronal cell bodies and dendrites. Neuroscience *55*, 463–472.

Frost, J.A., Geppert, T.D., Cobb, M.H., and Feramisco, J.R. (1994). A requirement for extracellular signal-regulated kinase (ERK) function in the activation of AP-1 by Ha-Ras, phorbol 12-myristate 13-acetate, and serum. Proc. Natl. Acad. Sci. USA *91*, 3844–3848.

Gotoh, Y., Nishida, E., Matsuda, S., Shiina, N., Kosako, H., Shiokawa, K., Akiyama, T., Ohta, K., and Sakai, H. (1991). In vitro effects on microtubule dynamics of purified *Xenopus* M phase-activated MAP kinase. Nature *349*, 251–254.

Grinnell, F., and Feld, M.K. (1982). Fibronectin adsorption on hydrophilic and hydrophobic surfaces detected by antibody binding and analyzed during cell adhesion in serum-containing medium. J. Biol. Chem. *257*, 4888–4893.

Grinstein, S., and Furuya, W. (1992). Chemoattractant-induced tyrosine phosphorylation and activation of microtubule-associated protein kinase in human neutrophils. J. Biol. Chem. *267*, 18122–18125.

Hanks, S.K., and Hunter, T. (1995). Protein kinases 6. The eukaryotic protein kinase superfamily: kinase (catalytic) domain structure and classification. FASEB J. *9*, 576–596.

Herzog, W., and Weber, K. (1978). Fractionation of brain microtubule-associated proteins. Isolation of two different proteins which stimulate tubulin polymerization in vitro. Eur. J. Biochem. *92*, 1–8.

Holt, K.H., Kasson, B.G., and Pessin, J.E. (1996). Insulin stimulation of a MEK-dependent but ERK-independent SOS protein kinase. Mol. Cell. Biol. *16*, 577–583.

Hoshi, M., Ohta, K., Gotoh, Y., Mori, A., Murofushi, H., Sakai, H., and Nishida, E. (1992). Mitogen-activated-protein-kinase-catalyzed phosphorylation of microtubule-associated proteins, microtubule-associated protein 2 and microtubule-associated protein 4, induces an alteration in their function. Eur. J. Biochem. *203*, 43–52.

Joneson, T., White, M.A., Wigler, M.H., and Bar-Sagi, D. (1996). Stimulation of membrane ruffling and MAP kinase activation by distinct effectors of RAS. Science *271*, 810–812.

Karin, M. (1995). The regulation of AP-1 activity by mitogen-activated protein kinases. J. Biol. Chem. *270*, 16483–16486.

Khalil, R.A., Menice, C.B., Wang, C.L., and Morgan, K.G. (1995). Phosphotyrosine-dependent targeting of mitogen-activated protein kinase in differentiated contractile vascular cells. Circ. Res. *76*, 1101–1108.

Lu, Q., Soria, J.P., and Wood, J.G. (1993). $p44^{mpk}$ MAP kinase induces Alzheimer type alterations in tau function and in primary hippocampal neurons. J. Neurosci. Res. *35*, 439–444.

Mandelkow, E.M., Drewes, G., Biernat, J., Gustke, N., Van Lint, J., Vandenheede, J.R., and Mandelkow, E. (1992). Glycogen synthase kinase-3 and the Alzheimer-like state of microtubule-associated protein tau. FEBS Lett. *314*, 315–321.

Mansour, S.J., Matten, W.T., Hermann, A.S., Candia, J.M., Rong, S., Fukasawa, K., Vande Woude, G.F., and Ahn, N.G. (1994). Transformation of mammalian cells by constitutively active MAP kinase kinase. Science *265*, 966–970.

Minden, A., Lin, A., Claret, F.X., Abo, A., and Karin, M. (1995). Selective activation of the JNK signaling cascade and c-Jun transcriptional activity by the small GTPases Rac and Cdc42Hs. Cell *81*, 1147–1157.

Morishima-Kawashima, M., and Kosik, K. (1996). The pool of MAP kinase associated with microtubules is small but constitutively active. Mol. Biol. Cell *7*, 893–905.

Nobes, C.D., and Hall, A. (1995). Rho, rac, and cdc42 GTPases regulate the assembly of multimolecular focal complexes associated with actin stress fibers, lamellipodia, and filopodia. Cell *81*, 53–62.

Noguchi, T., Metz, R., Chen, L., Matt'ei, M.G., Carrasco, D., and Bravo, R. (1993). Structure, mapping, and expression of *erp*, a growth factor-inducible gene encoding a nontransmembrane protein tyrosine phosphatase, and effect of ERP on cell growth. Mol. Cell. Biol. *13*, 5195–5205.

Pagès, G., Lenormand, P., L'Allemain, G., Chambard, J.C., Meloche, S., and Pouysségur, J. (1993). Mitogen-activated protein kinases $p42^{mapk}$ and $p44^{mapk}$ are required for fibroblast proliferation. Proc. Natl. Acad. Sci. USA *90*, 8319–8323.

Pillinger, M.H., Feoktistov, A.S., Capodici, C., Solitar, B., Levy, J., Oei, T.T., and Philips, M.R. (1996). Mitogen-activated protein kinase in neutrophils and enucleate neutrophil cytoplasts: evidence for regulation of cell-cell adhesion. J. Biol. Chem. *271*, 12049–12056.

Redwood, C.S., Marston, S.B., and Gusev, N.B. (1993). The functional effects of mutations $Thr^{673} \rightarrow Asp$ and $Ser^{702} \rightarrow Asp$ at the Pro-directed kinase phosphorylation sites in the C-terminus of chicken gizzard caldesmon. FEBS Lett. *327*, 85–89.

Reszka, A.A., Seger, R., Diltz, C.D., Krebs, E.G., and Fischer, E.H. (1995). Association of mitogen-activated protein kinase with the microtubule cytoskeleton. Proc. Natl. Acad. Sci. USA *92*, 8881–8885.

Ridley, A.J., and Hall, A. (1992). The small GTP-binding protein rho regulates the assembly of focal adhesions and actin stress fibers in response to growth factors. Cell *70*, 389–399.

Ridley, A.J., Paterson, H.F., Johnston, C.L., Diekmann, D., and Hall, A. (1992). The small GTP-binding protein rac regulates growth factor-induced membrane ruffling. Cell *70*, 401–410.

Robbins, D.J., Zhen, E., Owaki, H., Vanderbilt, C.A., Ebert, D., Geppert, T.D., and Cobb, M.H. (1993). Regulation and properties of extracellular signal-regulated protein kinases 1 and 2 in vitro. J. Biol. Chem. *268*, 5097–5106.

Robinson, M.J., Harkins, P.C., Zhang, J., Baer, R., Haycock, J.W., Cobb, M.H., and Goldsmith, E.J. (1996). Mutation of position 52 in ERK2 creates a nonproductive binding mode for adenosine 5′-triphosphate. Biochemistry *35*, 5641–5646.

Rozakis Adcock, M., van der Geer, P., Mbamalu, G., and Pawson, T. (1995). MAP kinase phosphorylation of mSos1 promotes dissociation of mSos1-Shc and mSos1-EGF receptor complexes. Oncogene *11*, 1417–1426.

Seger, R., Seger, D., Reszka, A.A., Munar, E.S., Eldar Finkelman, H., Dobrowolska, G., Jensen, A.M., Campbell, J.S., Fischer, E.H., and Krebs, E.G. (1994). Overexpression of mitogen-activated protein kinase kinase (MAPKK) and its mutants in NIH 3T3 cells. Evidence that MAPKK involvement in cellular proliferation is regulated by phosphorylation of serine residues in its kinase subdomains VII and VIII. J. Biol. Chem. *269*, 25699–25709.

Shiina, N., Moriguchi, T., Ohta, K., Gotoh, Y., and Nishida, E. (1992). Regulation of a major microtubule-associated protein by MPF and MAP kinase. EMBO J. *11*, 3977–3984.

Stossel, T.P. (1993). On the crawling of animal cells. Science *260*, 1086–1094.

Thompson, H.L., Shiroo, M., and Saklatvala, J. (1993). The chemotactic factor N-formylmethionyl-leucyl-phenylalanine activates microtubule-associated protein 2 (MAP) kinase and a MAP kinase kinase in polymorphonuclear leucocytes. Biochem. J. *290*, 483–488.

Verlhac, M.H., de Pennart, H., Maro, B., Cobb, M.H., and Clarke, H.J. (1993). MAP kinase becomes stably activated at metaphase and is associated with microtubule-organizing centers during meiotic maturation of mouse oocytes. Dev. Biol. *158*, 330–340.

Verlhac, M.H., Kubiak, J.Z., Clarke, H.J., and Maro, B. (1994). Microtubule and chromatin behavior follow MAP kinase activity but not MPF activity during meiosis in mouse oocytes. Development *120*, 1017–1025.

Verlhac, M.H., Kubiak, J.Z., Weber, M., G'Eraud, G., Colledge, W.H., Evans, M.J., and Maro, B. (1996). Mos is required for MAP kinase activation and is involved in microtubule organization during meiotic maturation in the mouse. Development *122*, 815–822.

Wang, X.M., Peloquin, J.G., Zhai, Y., Bulinski, J.C., and Borisy, G.G. (1996). Removal of MAP4 from microtubules in vivo produces no observable phenotype at the cellular level. J. Cell Biol. *132*, 345–357.

Wary, K.K., Maniero, F., Isakoff, S.J., Marcantonio, E.E., and Giancotti, F.G. (1996). The adaptor protein Shc couples a class of integrins to the control of cell cycle progression. Cell *87*, 733–743.

Waters, S.B., Holt, K.H., Ross, S.E., Syu, L.J., Guan, K.L., Saltiel, A.R., Koretzky, G.A., and Pessin, J.E. (1995). Desensitization of Ras activation by a feedback disassociation of the SOS-Grb2 complex. J. Biol. Chem. *270*, 20883–20886.

Worthen, G.S., Avdi, N., Buhl, A.M., Suzuki, N., and Johnson, G.L. (1994). FMLP activates Ras and Raf in human neutrophils. Potential role in activation of MAP kinase. J. Clin. Invest. *94*, 815–823.

Zhang, F., Strand, A., Robbins, D., Cobb, M.H., and Goldsmith, E.J. (1994). Atomic structure of the MAP kinase ERK2 at 2.3 A resolution. Nature *367*, 704–711.

Zhang, J., Zhang, F., Ebert, D., Cobb, M.H., and Goldsmith, E.J. (1995). Activity of the MAP kinase ERK2 is controlled by a flexible surface loop. Structure *3*, 299–307.

Zhang, S., Han, J., Sells, M.A., Chernoff, J., Knaus, U.G., Ulevitch, R.J., and Bokoch, G.M. (1995). Rho family GTPases regulate p38 mitogen-activated protein kinase through the downstream mediator Pak1. J. Biol. Chem. *270*, 23934–23936.